Journal of Cell Science 111, 199-211 (1998)
Printed in Great Britain © The Company of Biologists Limited 1998
JCS1488

EGF stimulates an increase in actin nucleation and filament number at the leading edge of the lamellipod in mammary adenocarcinoma cells

Amanda Y. Chan*, Steven Raft, Maryse Bailly, Jeffrey B. Wyckoff, Jeffrey E. Segall and John S. Condeelis

Department of Anatomy and Structural Biology, Albert Einstein College of Medicine, 1300 Morris Park Avenue, Bronx, NY 10461, USA
*Author for correspondence (e-mail: achan@aecom.yu.edu)
The data in this paper will be submitted in partial fulfillment of the requirement for the Degree of Doctor of Philosophy in the Sue Golding Graduate Division of Medical Sciences, Albert Einstein College of Medicine, Bronx, New York, USA

Accepted 11 November 1997: published on WWW 23 December 1997

SUMMARY

Stimulation of metastatic MTLn3 cells with EGF causes the rapid extension of lamellipods, which contain a zone of F-actin at the leading edge. In order to establish the mechanism for accumulation of F-actin at the leading edge and its relationship to lamellipod extension in response to EGF, we have studied the kinetics and location of EGF-induced actin nucleation activity in MTLn3 cells and characterized the actin dynamics at the leading edge by measuring the changes at the pointed and barbed ends of actin filaments upon EGF stimulation of MTLn3 cells. The major result of this study is that stimulation of MTLn3 cells with EGF causes a transient increase in actin nucleation activity resulting from the appearance of free barbed ends very close to the leading edge of extending lamellipods. In addition, cytochalasin D causes a significant decrease in the total F-actin content in EGF-stimulated cells, indicating that both actin polymerization and depolymerization are stimulated by EGF. Pointed end incorporation of rhodamine-labeled actin by the EGF stimulated cells is 2.12±0.47 times higher than that of control cells. Since EGF stimulation causes an increase in both barbed and pointed end incorporation of rhodamine-labeled actin in the same location, the EGF-stimulated nucleation sites are more likely due either to severing of pre-existing filaments or de novo nucleation of filaments at the leading edge thereby creating new barbed and pointed ends. The timing and location of EGF-induced actin nucleation activity in MTLn3 cells can account for the observed accumulation of F-actin at the leading edge and demonstrate that this F-actin rich zone is the primary actin polymerization zone after stimulation.

Key words: Actin nucleation, EGF, Metastasis, Motility

INTRODUCTION

Chemotaxis plays an important role in many basic biological processes including embryogenesis, neurite growth, wound healing, inflammation and cancer metastasis. Studies with highly motile cells such as *Dictyostelium* (Hall et al., 1989; Condeelis, 1993), neutrophils (Carson et al., 1986; Zigmond, 1996) and platelets (Hartwig et al., 1995) in particular have shown that stimulation of cells with chemoattractant generates a transient increase in actin nucleation activity in the actin cytoskeleton. It is unclear how stimulation of cell surface receptors is linked to actin polymerization. Actin polymerization could be stimulated by severing or uncapping of pre-existing actin filaments, increasing availability of polymerization competent monomeric actin, or by de novo assembly of new filaments (Condeelis, 1993; Zigmond, 1996).

EGF is a chemoattractant for MTLn3 cells, a metastatic cell line derived from the 13762 NF rat mammary adenocarcinoma (Neri et al., 1982). MTLn3 cells rapidly extend F-actin filled lamellipods in response to stimulation with EGF (Segall et al., 1996). Lamellipod extension begins within 1 minute after addition of EGF and becomes maximal by 3 minutes after stimulation. Optimum lamellipod extension occurs at about 5 nM EGF, near the K_d of the binding of EGF to its receptor. Microchemotaxis chamber measurements also demonstrate that the chemotactic and chemokinetic responses of MTLn3 cells are greatest at 5 nM EGF (Segall et al., 1996). Actin polymerization is necessary for these EGF-stimulated responses because cytochalasin D inhibits the EGF-stimulated lamellipod extension, increases in F-actin in lamellipods, and chemotaxis. There is no significant change in the total F-actin content after a 3 minute stimulation with EGF compared to control cells, suggesting that either new actin polymerization was terminated by 3 minutes, or that actin polymerization is exactly balanced by actin depolymerization (Segall et al., 1996).

Well characterized chemoattractants for amoeboid phagocytes such as cAMP, fMLP and autocrine motility factor act through G-protein coupled receptors (Devreotes and Zigmond, 1988; Silletti and Raz, 1993; Stracke et al., 1993). However, chemoattractants for cells derived from mesenchymal and epithelial tissues, such as EGF, act through receptors that are receptor tyrosine kinases (Hoelting et al., 1994; Pedersen et al., 1994; Wang et al., 1994; Royce and Baum, 1991; Grotendorst et al., 1989; Blay and Brown, 1985). Most studies on EGF-

stimulated signal transduction have been done on A431 cells (Boonstra et al., 1995; Peppelenbosch et al., 1993; Dadabay et al., 1991). Previous studies on EGF-induced reorganization of the actin cytoskeleton in A431 cells demonstrate the massive accumulation of F-actin and EGF-R in ruffles and under the plasma membrane at the free cell edge in colonies of A431 cells. F-actin content continues to increase with time after EGF addition in A431 cells (Rijken et al., 1991, 1995). Lipoxygenase and cycloxygenase products (Peppelenbosch et al., 1993) but not phosphoinositide turnover (Dadabay et al., 1991) are involved in EGF-induced remodeling of the actin cytoskeleton in A431 cells. These results are consistent with the observation that the EGF-R is an actin binding protein (den Hartigh et al., 1992) and that an EGF-R F-actin association may facilitate formation of a signaling complex containing other kinases and PLC in A431 cells (Diakonova et al., 1995; van Delft et al., 1995).

Although A431 cells are useful for studies of signal transduction, A431 cells are neither highly metastatic nor motile and express abnormally high levels of EGF-R (Price et al., 1988). MTLn3 cells on the other hand have high metastatic potential (Welch et al., 1983), are chemotactic to EGF (Segall et al., 1996) and the cell surface receptor for EGF is expressed at normal levels (Kaufmannn et al., 1990; Lichtner et al., 1992). In addition, the motile and chemotactic responses of MTLn3 cells have similarities to those seen in well-characterized cells such as *Dictyostelium* and neutrophils (Segall et al., 1996). Thus MTLn3 cells provide a powerful model system for the study of EGF-R involvement in cell motility, metastasis and tumor cell chemotaxis.

The relationship between EGF-induced signal transduction and cortical actin reorganization in MTLn3 and A 431 cells is presently unclear. Although A431 cells have been used to show that the EGF receptor is an actin binding protein and that stimulation with EGF stimulates an accumulation of F-actin under the plasma membrane, no studies have been done to address the underlying mechanism of EGF-stimulated actin reorganization. For example, does the EGF-stimulated accumulation of actin filaments at the leading edge of the lamellipod (Segall et al., 1996) result from new actin polymerization? If so, when and where does this polymerization occur? In this paper, we examined in detail the temporal and spatial distribution of actin polymerization in EGF-stimulated MTLn3 cells and characterized the actin dynamics by measuring the changes at the pointed and barbed ends of actin filaments upon EGF stimulation of MTLn3 cells. We used a pyrene-labeled actin nucleation assay to determine the kinetics of the nucleation activity in EGF-stimulated MTLn3 cells and an in situ rhodamine-labeled actin polymerization assay to determine the location of these nucleation sites.

MATERIALS AND METHODS

Cell culture

MTLn3 cells (kindly provided by Dr G. Nicolson, M. D. Anderson Cancer Center, Houston, Texas) were clonally derived from a lung metastasis of the 13762NF rat mammary adenocarcinoma (Neri et al., 1982). MTLn3 cells were grown to 60-80% confluence in minimal essential medium (Gibco MEM 12560) supplemented with 5% bovine serum as described in detail elsewhere (Segall et al., 1996).

Preparation of pyrene-labeled actin

Pyrene-labeled actin was prepared by reacting rabbit muscle actin with N-(1-pyrenyl)iodoacetamide as described by Cooper et al. (1983) except that the reagent was dissolved in DMSO. Pyrene labeled and unlabeled G-actin were chromatographed on Sephadex G150 (Pharamcia Fine Chemicals, Piscataway, NJ) before use. Both pyrene labeled and unlabeled G-actin were stored by dialysis against buffer A (2 mM Tris-HCl, 0.2 mM ATP, 0.5 mM DTT, 0.2 mM $CaCl_2$) at an approximate concentration of 20 μM.

Pyrene-labeled actin nucleation assay

Cells were harvested with 10 mM EDTA in serum-free MEMH (MEM in 12 mM Hepes, pH 7.4), centrifuged for 5 minutes at 4°C, 1,000 ***g*** and resuspended to a concentration of 1.75-2.0 million cells/ml in MEMH supplemented with 0.35% bovine serum albumin (buffer).

The cell suspension was equilibrated in a 37°C water bath for 10 minutes with occasional mixing of the tube by hand. Within 15 minutes of their removal from the substratum, control cells were treated with buffer, and experimental cells with a final concentration of 5 nM EGF (Life Technologies). The stock of EGF was prepared in filtered Dulbecco's PBS. At various times after treatment of cells with EGF or buffer, one part cell suspension was lysed directly in a spectrofluorometer cuvette held at 22°C and containing four parts lysis buffer (88 mM KCl, 5 mM DTT, 20 mM Pipes, pH 7.0, 1 mM ATP, 10 mg/ml BSA, 1 μg/ml chymostatin, leupeptin, and pepstatin, 5 mM EGTA, 0.2 mM $MgCl_2$, and 0.5% Triton X-100). Within 5 seconds, a mixture of 10% pyrene labeled and 90% unlabeled G-actin was added to cell lysates at a final concentration of 2 μM. Fluorescence was measured in a spectrofluorometer (F2000, Hitachi Corp.) at 22°C with an excitation wavelength of 365 nm (slit width 5 nm) and an emission wavelength of 407 nm (slit width 5 nm). Samples were exposed to the excitation beam intermittently and through a neutral density filter to avoid photobleaching. Cell lysates had no measurable autofluorescence at these wavelengths.

The initial rate of pyrene fluorescence increase was measured as the increase in fluorescence intensity over 10 minutes. The increase in fluorescence intensity was linear for the duration of the measurement. The relative rate was measured as the ratio of the initial rate of polymerization in the stimulated state relative to that in the unstimulated state. The unstimulated samples used for calculating were obtained by lysing cells prior to addition of EGF to the cell suspension.

In experiments involving use of cytochalasin D, the drug or DMSO was added to each cuvette 1 minute prior to the addition of cells. Cytochalasin D was added to a final concentration of 100 nM from a 25 μM stock prepared in DMSO. The number of barbed ends was determined by subtracting the raw rate in the presence of 0.1 μM cytochalasin D from the total rate. The number of barbed ends was calculated by converting the change in fluorescence of pyrene-labeled actin to concentration of F-actin using a standard curve and dividing the rate of change in concentration of F-actin by $(k_+ c - k_-)$ where C=2 μM, k_+=11.6/μM second and k_-=1.4/second (Pollard et al., 1983).

F-actin content in adherent and suspended cells

For quantification of F-actin in adherent MTLn3 cells using NBD-phallicidin, cells (2×10^5) were plated 18 hours before the beginning of the experiment. The cells were serum starved for 3 hours and then stimulated with 5 nM EGF for the appropriate amount of time. The cells were then fixed with 3.7% formaldehyde for 5 minutes in Buffer F (5 mM KCl, 138 mM NaCl, 4 mM $NaHCO_3$, 0.4 mM KH_2PO_4, 1.1 mM Na_2 HPO_4, 2 mM $MgCl_2$, 2 mM EGTA, 5 mM Pipes, pH 7.2) and then permeabilized with 0.5% Triton X-100 in Buffer F for 20 minutes. After a 10 minute rinse in 0.1 M gycline and 5 quick rinses with Buffer F, the cells were incubated in 1 μM NBD-phallicidin in Buffer F for 1 hour. Cells were washed 5× 5 minutes in Buffer F and the bound NBD-phallicidin was extracted using 100% methanol at 4°C for 90 minutes. After extraction, the methanol was removed and plated cells were washed 6× 5 minutes with Buffer F and a BCA assay was performed at 37°C for 30 minutes to determine total cell protein in the sample. Fluorescence of the methanol extraction solution for

each sample was recorded at 465 nm excitation and 535 nm emission, and normalized against cell protein. Numbers were expressed as relative F-actin content where:

$$\text{F-actin}\Delta_t/\text{F-actin}_0 = (\text{fluorescence}\Delta_t/\text{mg per ml})/(\text{fluorescence}_0/\text{mg per ml}).$$

The experiment was also done by pre-treating the cells with 100 nM cytochalasin D in MEMH for 1 minute prior to stimulation.

For quantification of F-actin in MTLn3 cells in suspension, the cells were serum starved for 2.5 hours, rinsed with 2 ml of 10 mM EDTA/MEMH, and incubated in 10 mM EDTA/MEMH for 30 minutes to get cells in suspension. Cells were spun at 1,000 ***g*** for 5 minutes and resuspended in MEMH at a density of 2×10^6 cells/ml. Cells were stimulated with 5 nM EGF at 37°C and at appropriate time points 1 ml was removed and added to 0.5 ml of 3× Buffer F with 11% formaldehyde and fixed for 15 minutes on a rotator at room temperature. The fixed cells were centrifuged in a microcentrifuge for 1 minute and resuspended in 0.5 ml Buffer F with 0.1% saponin and 1 μM NBD-phallicidin. Cells were stained on a rotator for 1 hour at room temperature. Cells were pelleted as before and rinsed in 1 ml Buffer F, repelleted, and resuspended in 100% methanol and extracted on a rotator for 90 minutes at room temperature. The cells were again pelleted and the methanol was removed to a new tube. The NBD-phallicidin fluorescence in the methanol extract was read using a fluorimeter at 465 nm excitation and 535 nm emission. Numbers were normalized to the reading for control cells.

Preparation of rhodamine- and biotin-labeled-actin

Rhodamine-labeled actin was prepared by reacting rabbit muscle actin with 5- (and) 6-carboxytetramethylrhodamine, succinimidylester (NHSR, Molecular Probes c-1171). Two cycles of actin assembly-disassembly were performed to characterize the rhodamine-labeled actin. 39 mg of Spudich and Watt actin (Spudich et al., 1971) were dialyzed against two changes of 250 ml of 5 mM Tris-HCl, pH 8, 0.2 mM $CaCl_2$ and 0.2 mM ATP for 24 hours. G-actin was then clarified and diluted to 3 mg/ml with 50 mM K Pipes, pH 6.8, 50 mM KCl, 0.2 mM $CaCl_2$, and 0.2 mM ATP (buffer B). G-actin was polymerized by dialyzing it against 1,000 ml of buffer B for 3 hours. F-Actin was then dounced on ice to break up aggregates, ATP was added to 0.5 mM and NHSR was added to a concentration of 0.625 mg/ml. The reaction mixture was incubated at room temperature in the dark for 1 hour and F-actin was pelleted by spinning for 2 hours in a Ti 70 rotor (Beckman) at 48,000 rpm at 4°C. The pellet was resuspended and dounced on ice with 2 ml of 20 mM Tris-HCl, pH 8.1, 5 mM DTT, 5 mM K glutamate, 0.2 mM $CaCl_2$ and 1 mM ATP and 1 ml of buffer A, 2 mM Tris-HCl, 0.2 mM ATP, 0.5 mM DTT, 0.2 mM $CaCl_2$ and 0.02% sodium azide. Actin filaments were dialyzed against buffer A for 48 hours to depolymerize the filaments. G-actin was clarified in a TL100 rotor at 95, 000 rpm for 15 minutes at 4°C and chromatographed over a G-150 column that was previously equilibrated with buffer A. The G-actin from the protein pool was polymerized with 10 mM Pipes, pH 7, 2 mM $MgCl_2$ and 50 mM KCl at room temperature for 1 hour. F-Actin was pelleted in a Ti 70 rotor at 48,000 rpm at 4°C for 2 hours, resuspended in 5 ml of buffer A and dialyzed for 2 days on ice against buffer A. Another cycle of actin assembly and disassembly was carried out as described to characterize the rhodamine-labeled actin and demonstrate that the dye:protein ratio remained constant. The dye to protein ratio was determined by absorption spectrophotometry using extinction coefficients of ε_{280}=48,988/M cm for actin and ε_{560}=50,000/M cm for tetramethyl rhodamine (Molecular Probes). The final G-actin was dialyzed against 1 M sucrose in buffer A for 6 hours and stored frozen in liquid nitrogen. The frozen rhodamine-labeled actin stock was stored at a concentration of 237 μM with a dye to protein ratio of approximately 1 to 1.

Biotin-labeled actin was prepared as described for rhodamine-actin using *N*-hydroxysuccinimidobiotin (Pierce).

Saponin permeabilization of MTLn3 cells

MTLn3 cells were plated on collagen I coated MATTEK tissue culture dishes for 24 hours. Cells were plated at a density of 5,000 cells/cm^2 and incubated overnight in complete growth medium including 5% FCS as described above. On the day of the experiment, the cells were serum starved for 3 hours in a serum free buffer (MEMH supplemented with 0.35% BSA). Stock rhodamine-labeled actin was rapidly thawed from liquid nitrogen and diluted to 12 μM with 1 mM Hepes, pH 7.5, 0.2 mM $MgCl_2$, and 0.2 mM ATP, sonicated and clarified in a airfuge for 20 minutes. Control cells were treated with buffer, and experimental cells with a final concentration of 5 nM EGF in buffer for various times at 37°C. Further steps were done at room temperature. The stimulation medium was aspirated and cells were permeabilized with permeabilization buffer (PB)(20 mM Hepes, pH 7.5, 138 mM KCl, 4 mM $MgCl_2$, 3 mM EGTA, 0.2 mg/ml of saponin, 1 mM ATP, 1% BSA) containing 0.45 μM or 2 μM rhodamine-labeled actin that was added just before application to cells. At various times after incubation with PB containing rhodamine-labeled actin, cells were fixed for 5 minutes with 3.7% formaldehyde in PBS (145 mM NaCl, 4 mM NaH_2PO_4, 6 mM Na_2 $HPO_4.7H_2O$ and 0.02% NaN_3). This was then replaced with 0.1 M glycine in PBS for 10 minutes. After washing the cells 5× with PBS, the cells were stained with 1 M fluorescein phalloidin for 20 minutes in a humidified chamber. Unbound stain was then washed off with PBS 5× and a coverslip was mounted on the MATTEK dish with 0.1 M *N*-propyl gallate, 0.02% NaN_3 in 50% glycerol in PBS, pH 7.0.

Capping protein from *Dictyostelium* (Eddy et al., 1996), kindly provided by Jing Hua Han, was kept at a stock concentration of 2 μM in mono Q buffer (20 mM Tris-HCl, pH 7.5, 35 mM NaCl, 0.5 mM DTT and 1 mM EGTA). Cytochalasin D was obtained from Sigma, and stored as a 2 μM stock in DMSO.

Experiments involving the use of gelsolin-actin complex

MTLn3 cells were lysed in PB containing 5 μM phallicidin for 1 minute, then washed in PB without saponin, and then incubated in 500 μl of 100 nM gelsolin-actin complex for 10 minutes to cap all existing free barbed ends. Control cells were incubated in parallel in 100 nM G-actin. After incubation, cells were rinsed in PB without saponin, then incubated with 500 μl of 2 μM rhodamine-labeled actin for various times. Gelsolin-actin complex (GA2) was prepared by incubating 5 μM of purified gelsolin (gift of Dr J. Hartwig) and 10 μM G-actin in 10 mM Tris-HCl, pH 8, 0.2 μM $CaCl_2$, 0.5 mM ATP, 50 μM CaEDTA, 1 mM DTT, 1 mM sodium azide, overnight at room temperature according to a protocol described by Redmond and Zigmond, (1993). The complex was stored at 4ºC and diluted 50-fold into PB without saponin.

The relative number of pointed ends was measured as an increase in the incorporation of 2 μM rhodamine-actin into GA2 capped cells. We have shown previously that the number of pointed ends estimated by this capping method gives identical results to pointed ends measured using the Dnase binding assay (Eddy et al., 1997).

Analysis

To observe cells that were labeled with rhodamine-labeled actin and stained with fluorescein phalloidin, fluorescence imaging and data collection was done using a SIT camera (Hamamatsu), ×60 objective (NA 1.4) on a Nikon Diaphot with fluorescence optics. Identical settings were used to collect images from cells at each of the experimental conditions being tested in the linear range of the detector's response and at a sensitivity such that none of the pixels in the image were saturated.

To quantitate the fluorescence as a function of distance from the edge of the lamellipod, data were collected for equal numbers of cells from each experimental condition tested. Images from the SIT camera were collected and stored on a Macintosh computer using NIH Image. Analysis of the images from the SIT camera was done by a macro program described previously that measures the fluorescence as a function of distance from the leading edge of the lamellipod (Segall et

al., 1996). Cells with well preserved lamellipods were selected, ruffling areas were excluded, a line was drawn parallel to the leading edge of the chosen lamellipod. The average pixel intensity beginning at the leading edge and extending 5 μm into the cells was measured using the macro. Since EGF stimulates an extension of a lamellipod on each cell that has rhodamine-labeled actin incorporation around the entire lamellipod, a line approximately 10 μm in length was drawn randomly on each EGF-stimulated lamellipod. Control cells had various rhodamine-labeled actin intensities at the leading edge. Therefore, two different measurements were done, one including only the brightest areas at the leading edge of the lamellipod and another measurement was done randomly within the leading edge of the lamellipod.

Confocal images were acquired with a NA 1.4 ×60 objective on Bio-Rad MRC-600 confocal microscope as single optical sections 0.5 μm from the substratum. Images of cells were first taken in the rhodamine channel using a rhodamine filter, then the same cells at the same focal plane were imaged with a fluorescein filter. The two images were taken with two different filter blocks to avoid cross channel fluorescence. The overlaying of the two images was done with the NIH image program.

For quantification of the pixel intensity of rhodamine-labeled actin after various rhodamine-labeled actin incubation times or various EGF stimulation times, the images were acquired from an Olympus microscope that is equipped with a Cooled CCD camera. Rhodamine-labeled actin incorporation at the cell edge was measured as the average pixel intensity of the area between the two lines shown in Fig. 5A and the average pixel intensity of the area inside the line shown in Fig. 5B is the measurement for the cell center.

Electron microscopy

MTLn3 cells were grown on Parlodion-carbon-coated gold square support grids on coverslips (Electron Microscopy Science, Fort Washington, PA) for 18-24 hours. The cells were starved for 3 hours in MEMH supplemented with 0.35% BSA, and then stimulated with 5 nM EGF for 1 minute. The coverslips were then treated with 0.25% Triton X-100 in buffer C (138 mM KCl, 10 nM Pipes, pH 6.9, 0.1 mM ATP, 3 mM EGTA, pH 6.9, 4 mM $MgCl_2$), 1% BSA and in the presence or absence of 0.45 μM G-actin for 1 minute. After a rapid wash in buffer C, the preparations were fixed with 1% glutaraldehyde in cytoskeletal buffer, pH 6-6.1 (5 mM KCl, 137 mM NaCl, 4 mM $NaHCO_3$, 0.4 mM KH_2PO_4, 1.1 mM Na_2HPO_4, 2 mM $MgCl_2$, 5 mM Pipes, 2 mM EGTA, 5.5 mM glucose) in the presence of 5 μM phallicidin for 15 minutes. The grids were then rinsed in cytoskeletal buffer and sequentially transferred through 4 drops of 40 μg/ml of bacitracin in water, followed by 4 drops of 1% phosphotungstic acid. The grids were then blotted dry and observed using a JEOL 100CX transmission electron microscope.

RESULTS

Actin nucleation activity in lysates varies with time after stimulation

Our previous studies have demonstrated that addition of EGF to MTLn3 cells stimulates extension of lamellipods that contain increased amounts of F-actin at the leading edge (Segall et al., 1996). To determine if there is a transient burst of actin polymerization after EGF stimulation that can account for this redistribution of F-actin, pyrene-labeled actin was used to measure the timing of actin nucleation after EGF stimulation of MTLn3 cells. Cells were lysed with Triton X-100 at various times after stimulation with EGF. The amount of nucleation activity present in the lysate at each time point was measured as an increase in fluorescence over the first 10 minutes, and expressed either as relative rate or initial rate (as described in Materials and Methods).

The relative rate of actin polymerization in lysates from

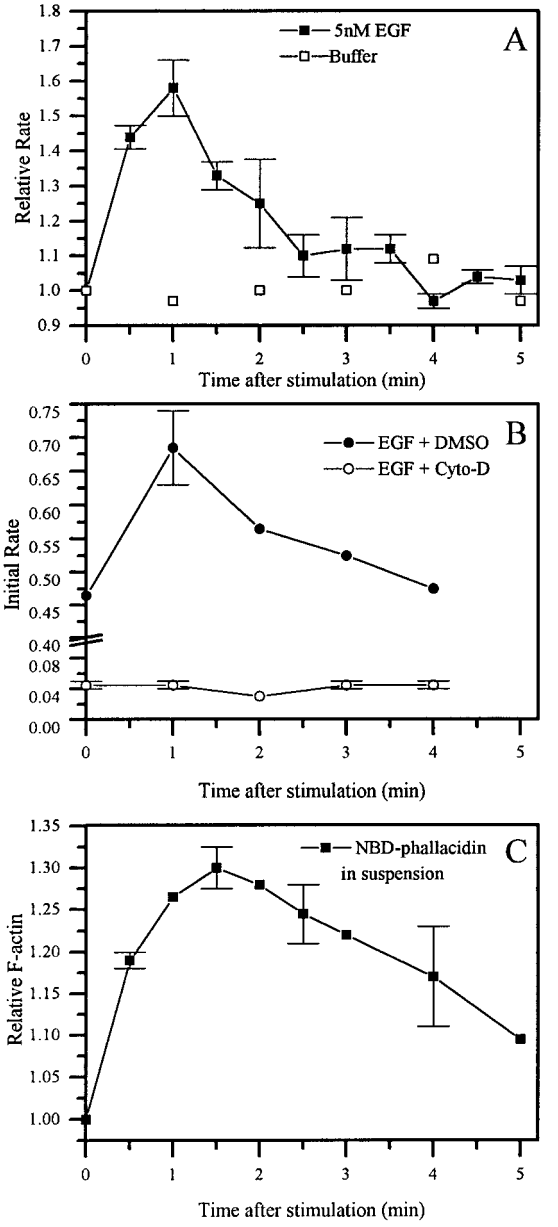

Fig. 1. EGF stimulates a cytochalasin-sensitive actin nucleation activity that occurs just preceding the increase in F-actin. (A) Actin nucleation activity in cell lysates varies with time after EGF-stimulation. (■) Data from EGF-stimulated cells; each point is the average of four independent experiments. (□) Data from control cells subjected to addition of buffer that does not contain EGF. Relative rate is the initial rate of actin polymerization in lysates from EGF-stimulated cells divided by the initial rate from the unstimulated cells in the same experiment. Error bars show s.e.m., n=4. (B) Cytochalasin D inhibits the elongation of actin filaments in lysates from both resting (t=0) and EGF-stimulated cells. The initial rate of polymerization of 2 μM pyrene actin is shown in cell lysates in which 100 nM cytochalasin D (○) or DMSO (●) was added to lysis buffer before the introduction of EGF-stimulated cells. Initial rate of actin polymerization was measured by following the fluorescence of pyrene-labeled actin over 10 minutes. Error bars are s.e.m., n=3. (C) The F-actin content of suspended MTLn3 cells increases transiently following EGF-stimulation. F-actin content was measured using the NBD-phallicidin binding assay. Error bars show s.e.m., n=3.

stimulated cells varies with time after stimulation, as shown in Fig. 1A. The relative rate peaks at one minute and decreases steadily reaching the pre-stimulated level at 4 minutes after EGF stimulation. The number of free barbed ends (calculated as described in Materials and Methods using the rate constants supplied there) increases by approximately 13,000 by 1 minute after EGF stimulation from 24,000 to 37,000 per cell. This represents a rate of 8×10^5 monomers/second per cell at rest and 1.2×10^6 monomers/second per cell at 1 minute after stimulation. Addition of buffer rather than EGF does not stimulate a significant increase in nucleation activity. The fluctuation (standard derivation) of the relative rate in control cells is 0.04 compared to the increase in rate in cells 1 minute after EGF stimulation. This result indicates that the variation in the background nucleation activity in control cells is small relative to the increase in nucleation activity in EGF stimulated cells.

Actin polymerization occurring in cell lysates from both resting and stimulated cells is effectively inhibited by 100 nM cytochalasin D. As shown in Fig. 1B there is a 90% decrease in the initial rate of pyrene actin polymerization in unstimulated cell lysates in the presence of cytochalasin D. In addition this inhibition is observed during EGF stimulation, suggesting that the nucleation activity results in filaments that grow at the preferred, i.e. barbed ends.

Studies from *Dictyostelium* (Hall et al., 1989) and neutrophils (Redmond and Zigmond, 1993) have shown that the increase in nucleation activity after stimulation is often accompanied by an increase in total F-actin content. To quantitate the F-actin content in MTLn3 cells in suspension, we used the NBD-phallicidin binding assay as described in Materials and Methods. As shown in Fig. 1C, the maximum increase in relative F-actin content occurred at 1.5 minutes after EGF stimulation, i.e. a time just after the peak of nucleation activity (at 1 minute). These results are consistent with a model in which the increase in the number of nucleation sites causes an increase in total polymer mass.

Rhodamine-labeled G-actin is incorporated preferentially at the leading edge of lamellipods induced by EGF stimulation

While the pyrene-labeled actin and NBD-phallicidin assays provide useful information on the time course of actin nucleation, they do not address the spatial organization of the EGF-stimulated nucleation sites in cells. To determine the location of nucleation sites, exogenous rhodamine-labeled actin was added to saponin-permeabilized MTLn3 cells in an experiment designed after the procedures of Symons and Mitchison (1991) and Redmond and Zigmond (1993). Exogenous rhodamine-labeled actin incorporates into the

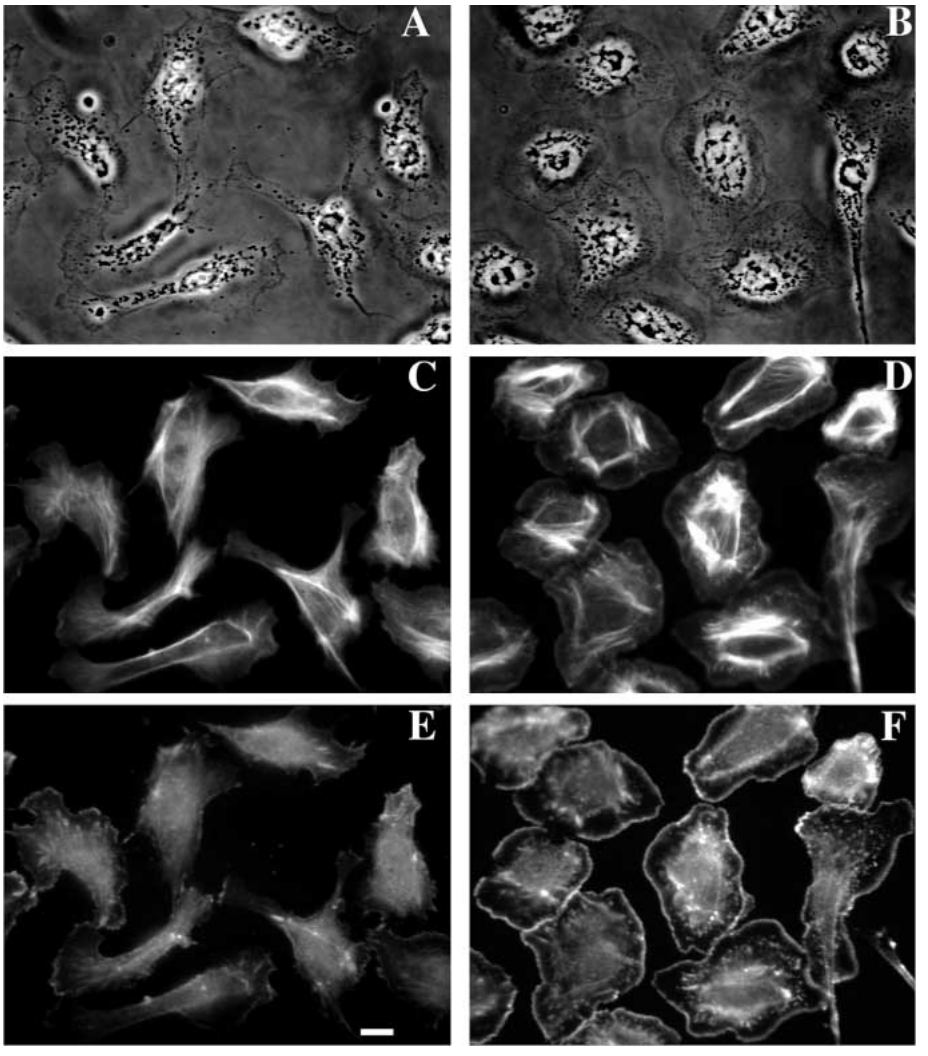

Fig. 2. Rhodamine-labeled actin polymerizes preferentially at the leading edge of lamellipods in EGF-stimulated cells. MTLn3 cells were stimulated for 1 minute with either buffer (A,C,E) or 5 nM EGF (B,D,F); permeabilized with 0.2 mg/ml saponin together with 0.45 μM rhodamine-labeled actin in permeabilization buffer and incubated for 5 minutes. Permeabilized cells were fixed and stained with fluorescein-phalloidin. (A,B) Phase-contrast; (C,D) fluorescein-phalloidin channel showing total F-actin; (E,F) rhodamine-labeled actin channel showing incorporated exogenous rhodamine-labeled actin. All images were obtained at identical settings in each channel. Bar, 10 μm.

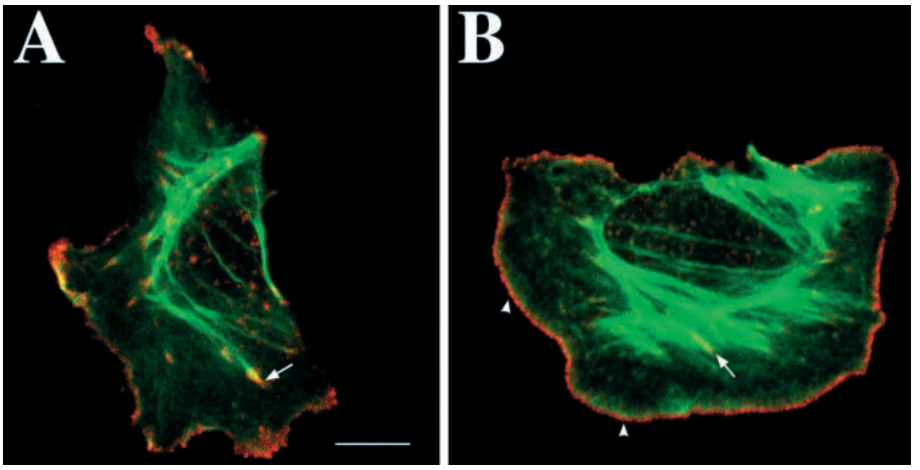

Fig. 3. EGF stimulates lamellipod extension and accumulation of F-actin and rhodamine-labeled actin at the leading edge of the lamellipod. This figure is an overlay image of the fluorescein-phalloidin(green) and rhodamine-labeled actin(red) channels from two confocal images. (A) Control cells have incorporated rhodamine-labeled actin only at sites of protrusive activity. (B) EGF-stimulated cells extend broad and almost encompassing lamellipods with intense and continuous rhodamine-labeled actin at the leading edge of the lamellipod. The rhodamine-labeled actin cortex as seen in red is more proximal to the plasma membrane than the broad green F-actin zone (arrowheads). Both EGF-stimulated and control cells have rhodamine-labeled actin incorporating at the ends of stress fibers (arrows). Bar, 10 μm.

exposed nucleation sites inside the cell, marking their location. In Figs 2 and 3, MTLn3 cells were treated with either buffer or 5 nM EGF for 1 minute, permeabilized in the presence of rhodamine-labeled actin monomers (which could then polymerize from the saponin-exposed nucleation sites) and then fixed and counter stained with fluorescein-phalloidin to visualize all actin filaments. Almost all cells stimulated with EGF extend around their entire periphery a flat, hyaline, ruffle-free lamellipod that is seen only occasionally in control cells (Fig. 2A,B). EGF inhibits ruffling and stimulates lamellipod extension simultaneously resulting in flattening of the cell edge as show by scanning electron microscopy elsewhere (J. B. Wyckoff, J. S. Condeelis and J. E. Segall, unpublished). FITC-phalloidin staining demonstrates that F-actin accumulates at the leading edge of these lamellipods in EGF-stimulated cells without significant changes in the rest of the cytoskeleton (Fig. 2C,D). In control cells, rhodamine-labeled actin incorporates primarily at the leading edge of spontaneously moving cells and at the ends of stress fibers (Figs 2E, 3A). However, in EGF-stimulated cells (Figs 2F, 3B) rhodamine-labeled actin shows dramatic incorporation along the entire lamellipod edge whereas incorporation in stress fibers is like that seen in control cells. Similar results were also observed in a control experiment where we permeabilized cells with 0.25% Triton X-100 instead of 0.2% saponin. In the Triton experiment, the exogenous labeled actin also preferentially incorporated at the leading edge of the lamellipod after EGF stimulation, similar to that observed in the saponin permeabilized cells (data not shown). In another experiment, we added 2 μM instead of 0.45 μM rhodamine-labeled actin to saponin permeabilized cells, in which case, an identical pattern of rhodamine-labeled actin incorporation was observed (data not shown).

To quantitate the morphological changes of MTLn3 cells in response to EGF, we scored the number of cells with lamellipods that contained F-actin localized to the lamellipod leading edge and lamellipods that contained a continuous rhodamine-labeled actin zone. As shown in Table 1, 43 out of 61 EGF-stimulated cells contained F-actin rich lamellipods, compared to 9 out of 64 control cells, and 58 out of 61 EGF-stimulated cells had continuous intense rhodamine fluorescence in the entire edge of the lamellipod compared to only 8 out of 64 control cells. When the rhodamine-labeled actin fluorescence was quantitated as a function of distance from the leading edge of the cells (as described in Materials and Methods), hyaline regions of the cell periphery showed more rhodamine-labeled actin staining near the plasma membrane in EGF stimulated cells as compared to the brightest area within the lamellipod of control cells (Fig. 4A). The difference in rhodamine-labeled actin incorporation between the control cells and stimulated cells is more apparent when the measurement is done randomly on the lamellipod of stimulated or control cells (Fig. 4A). As shown in Fig. 4B, the maximal ratio of rhodamine-labeled actin to F-actin at the leading edge changes upon EGF stimulation. The change in ratio induced by EGF stimulation is more apparent adjacent to the plasma membrane of the cells. The result shown in Fig. 4B compliments that shown in Fig. 3 where the comparison of the distribution of F-actin (green) and rhodamine-labeled actin (red) in 2 channel overlays demonstrates that the rhodamine-labeled actin is narrower and closer to the plasma membrane than the F-actin zone at the leading edge of the lamellipod. The distribution of stain indicates that the nucleation sites are more proximal to the plasma membrane side of the F-actin rich cortex.

To determine whether the pattern of rhodamine-labeled actin incorporation observed in EGF-stimulated MTLn3 cells is dependent on diffusion, the rhodamine fluorescence intensity at the leading edge of the lamellipod was compared to that in the cell center as a function of the rhodamine-labeled actin incubation time. Since the thickness of the cell differs between the center and the lamellipod leading edge, the time required for actin to diffuse throughout may be different for these two compartments. If rhodamine-labeled actin incorporation is

Table 1. Quantitation of morphological changes in response to EGF

Treatment	Lamellipods with F-actin leading edge*	Lamellipods with rhodamine-labeled actin leading edge†
Buffer	9/64	8/64
5 nM EGF	43/61	58/61

Six fields of cells as shown in Fig. 2 were counted. The total number of cells counted in all fields is the denominator.

*Cells were scored for lamellipods that contained F-actin localized to the leading edge as shown in Fig. 2D.

†Cells were scored for lamellipods that contained a continuous rhodamine-labeled actin zone as in Fig. 2F.

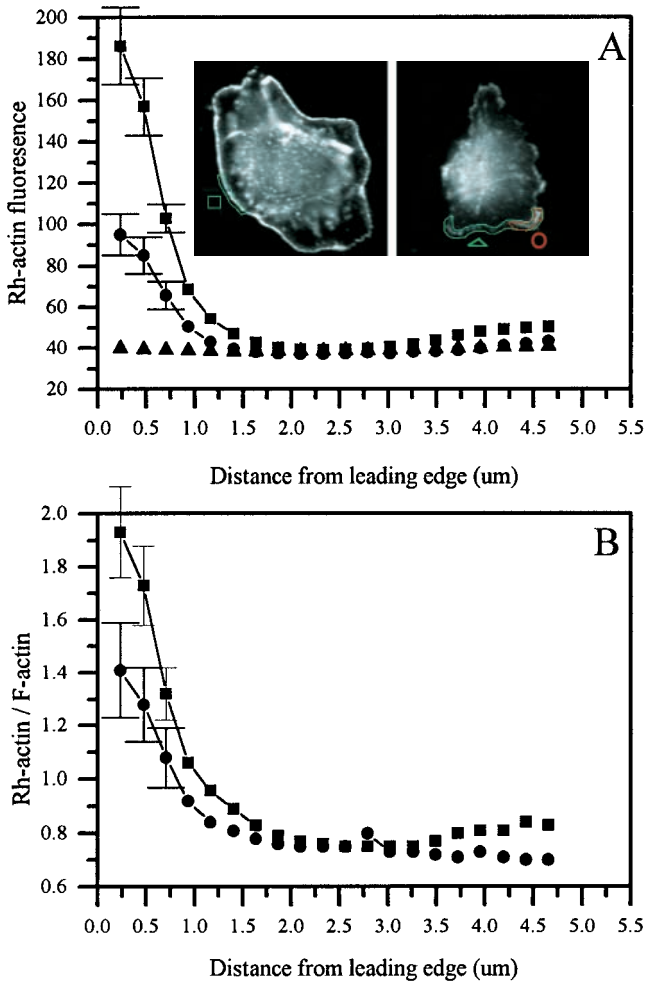

Fig. 4. Rhodamine-labeled actin fluorescence near the plasma membrane is brighter in EGF stimulated cells than control cells. Distribution of rhodamine-labeled actin fluorescence measured as a function of distance from the leading edge of the lamellipod. Measurements of 10 cells taken from SIT camera images. (■) Measurement of random lamellipod edges in cells stimulated with EGF for 1 minute. (●) Measurement of the brightest lamellipod area of control cells after treatment with buffer for 1 minute. (▲) Measurement of random lamellipod edges in control cells. Inset demonstrates the typical areas measured in EGF stimulated or control cells Error bars are s.e.m., *n*=10 cells. (B) Ratio of rhodamine-labeled actin to F-actin increases upon stimulation of EGF in MTLn3 cells. (■) MTLn3 cells after 1 minute EGF stimulation; (●) MTLn3 cells after 1 minute buffer treatment. The brightest area measurements were used for control cells. Error bars are s.e.m., *n*=10 cells.

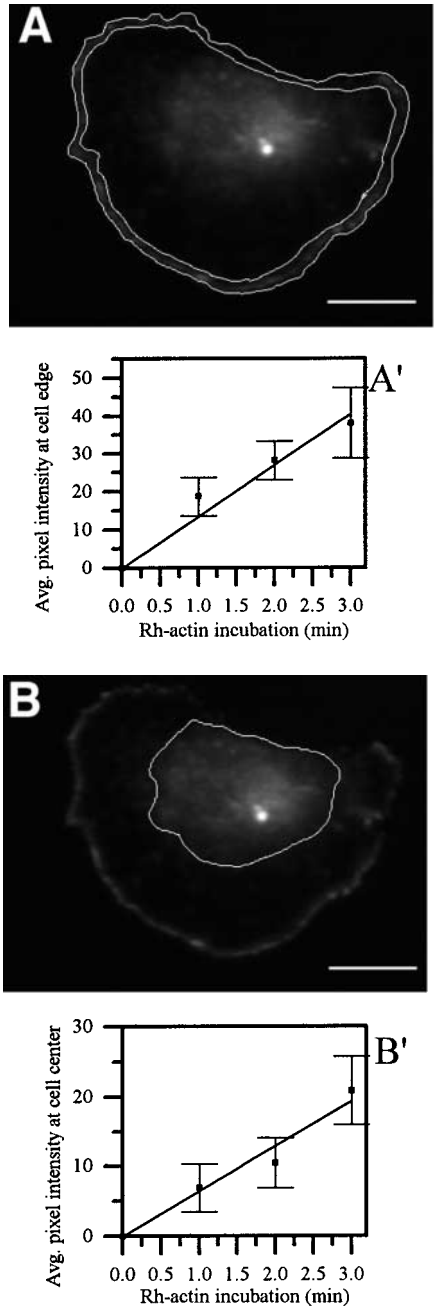

Fig. 5. Rhodamine-labeled actin incorporation in permeabilized MTLn3 cells is not diffusion limited. Changes in fluorescence intensity as a function of the incubation time: (A′) rhodamine-labeled actin intensity at the leading edge of the lamellipod; (B′) rhodamine-labeled actin intensity at the cell center. Data for each time point is the average and s.e.m. of 15 different cells. Images A and B are examples of where on cells the measurements were taken. Bars, 10 μm.

diffusion limited, polymerization of rhodamine-labeled actin at the leading edge of the lamellipod would be different from incorporation at the cell center. As shown in Fig. 5A′ and B′, rhodamine-labeled actin polymerization is linear within the 3 minutes of incubation used in these experiments for both the leading edge and cell center. Therefore, the pattern of rhodamine-labeled actin incorporation observed in EGF-stimulated MTLn3 cells is dependent on the availability of nucleation sites and not dependent on differences in cell thickness. This is also supported by Fig. 6, which shows that the same pattern of rhodamine-labeled actin incorporation is observed whether cells are incubated for 1 minute or 3 minutes with rhodamine-labeled actin.

EGF stimulates actin nucleation activity in cells plated on a surface

To compare the rhodamine-labeled actin incorporation sites

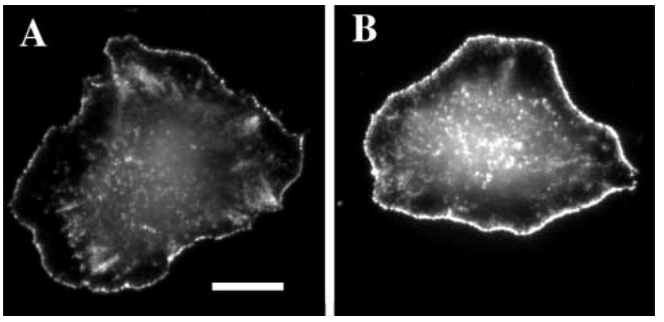

Fig. 6. The pattern of rhodamine-labeled actin incorporation in saponin permeabilized MTLn3 cells does not change over time. (A) Cells were stimulated with 5 nM EGF for 1 minute, incubated in permeabilization buffer containing 0.45 μM rhodamine-labeled actin for 1 minute or (B) for 3 minutes, fixed and viewed. Bar, 10 μm.

observed in MTLn3 cells with the nucleation activity observed in cell lysates, we repeated the rhodamine-labeled actin experiment over the time course done for the pyrene-labeled actin experiment. MTLn3 cells were stimulated for various times, permeabilized in the presence of 0.45 μM rhodamine-labeled actin for 2 minutes, fixed and fluorescent cells were visualized using an Olympus microscope equipped with a Cooled CCD camera. Fig. 7A shows the pattern of incorporation of rhodamine-labeled actin with cells stimulated for different times. Rhodamine-labeled actin fluorescence was quantitated by measuring the average pixel intensity at the leading edge as in Fig. 5A. Fig. 7B shows that the relative rate of rhodamine-labeled actin incorporation peaks at 1 minute after stimulation and decreases to prestimulation levels by 4 minutes. Therefore, cells in suspension and cells adherent to a surface show the same overall pattern of actin nucleation kinetics after EGF stimulation.

To quantitate the relative F-actin content of MTLn3 cells

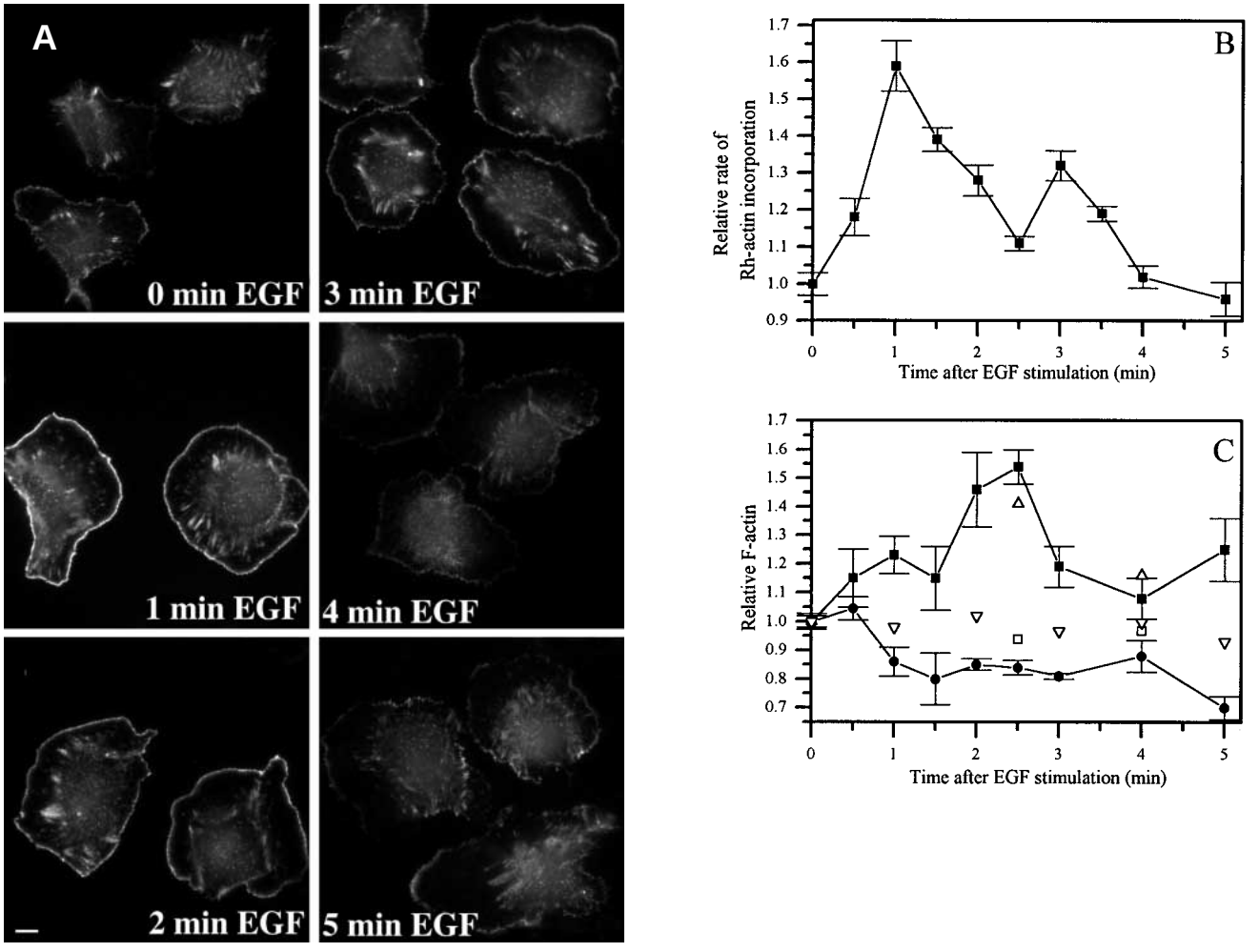

Fig. 7. Rhodamine-labeled actin incorporation from the barbed ends is maximal at 1 minute after EGF stimulation. (A) Images of rhodamine-labeled actin incorporation for MTLn3 cells stimulated for 0 to 5 minutes with 5 nM EGF. Bar, 6.3 μm. (B) Relative rate of rhodamine-labeled actin incorporation is the average pixel intensity at the cell edge of stimulated cells divided by that of unstimulated cells after 2 minutes of incubation with 0.45 μM rhodamine-labeled actin. The cell edge is defined as in Fig. 5A. Error bars are s.e.m., n=20 cells. (C) F-actin content of adherent MTLn3 cells increases transiently following EGF-stimulation. Relative F-actin content of MTLn3 after stimulation with EGF (■), buffer (□), EGF + 0.4% DMSO (△). EGF-stimulation induces a decrease in F-actin content in the presence of 100 nM cytochalasin D (●), a drop in F-actin content is not seen in unstimulated cells held in 100 nM cytochalasin D (▽). Error bars are s.e.m., n=3 experiments.

adherent to a surface, the NBD-phallicidin assay was done with cells plated on collagen (Fig. 7C). The relative F-actin content of adherent MTLn3 cells increases transiently, peaking at 2.5 minutes. This result is similar to that observed with cells in suspension in that the appearance of barbed ends (Fig. 7B) precedes the accumulation of F-actin (Fig. 7C). In the presence of 100 nM cytochalasin D, EGF stimulation induces a decrease in total F-actin content in whole cells. These results suggest that both polymerization and depolymerization are stimulated by EGF and that the depolymerization can be detected when polymerization is blocked by capping the barbed ends of filaments.

Actin nucleation in permeabilized MTLn3 cells is barbed end dependent

We used electron microscopy to visualize exogenous actin incorporation at the single filament level to determine if rhodamine-labeled actin incorporation is specific to preexisting filament ends. As shown in Fig. 8, polymerization of exogenous actin is only observed in association with pre-existing filaments in the cytoskeleton after EGF stimulation (Fig. 8B) while short actin filaments are not observed in the background in any case. These results indicate that the rhodamine-labeled actin fluorescence observed in MTLn3 cells results from polymerization in association with preexisting filaments in cells and not cross linking to the cytoskeleton of rhodamine-labeled actin filaments formed in the incubation buffer.

To determine whether the EGF-stimulated incorporation of rhodamine-labeled actin into the saponin cytoskeleton is dependent on pointed or barbed end subunit addition, we measured the effect of capping protein, which specifically caps the barbed ends of actin filaments. Cells were stimulated with 5 nM EGF for 1 minute, permeabilized in the presence or absence of 20 nM capping protein and subsequently incubated for 5 minutes with 0.45 μM rhodamine-labeled actin in permeabilization buffer, fixed and stained with fluorescein-phalloidin as before. Capping protein inhibits the incorporation of rhodamine-labeled actin at the leading edge of the lamellipods and at the ends of the stress fibers (data not shown). To study this further and to demonstrated that there is no cross-channel fluorescence in our imaging system, the above experiment was repeated with 100 nM cytochalasin D without the addition of fluorescein-phalloidin. As shown in Fig. 9C, in the absence of cytochalasin D, a similar pattern of rhodamine-labeled actin incorporation was observed in cells stained with

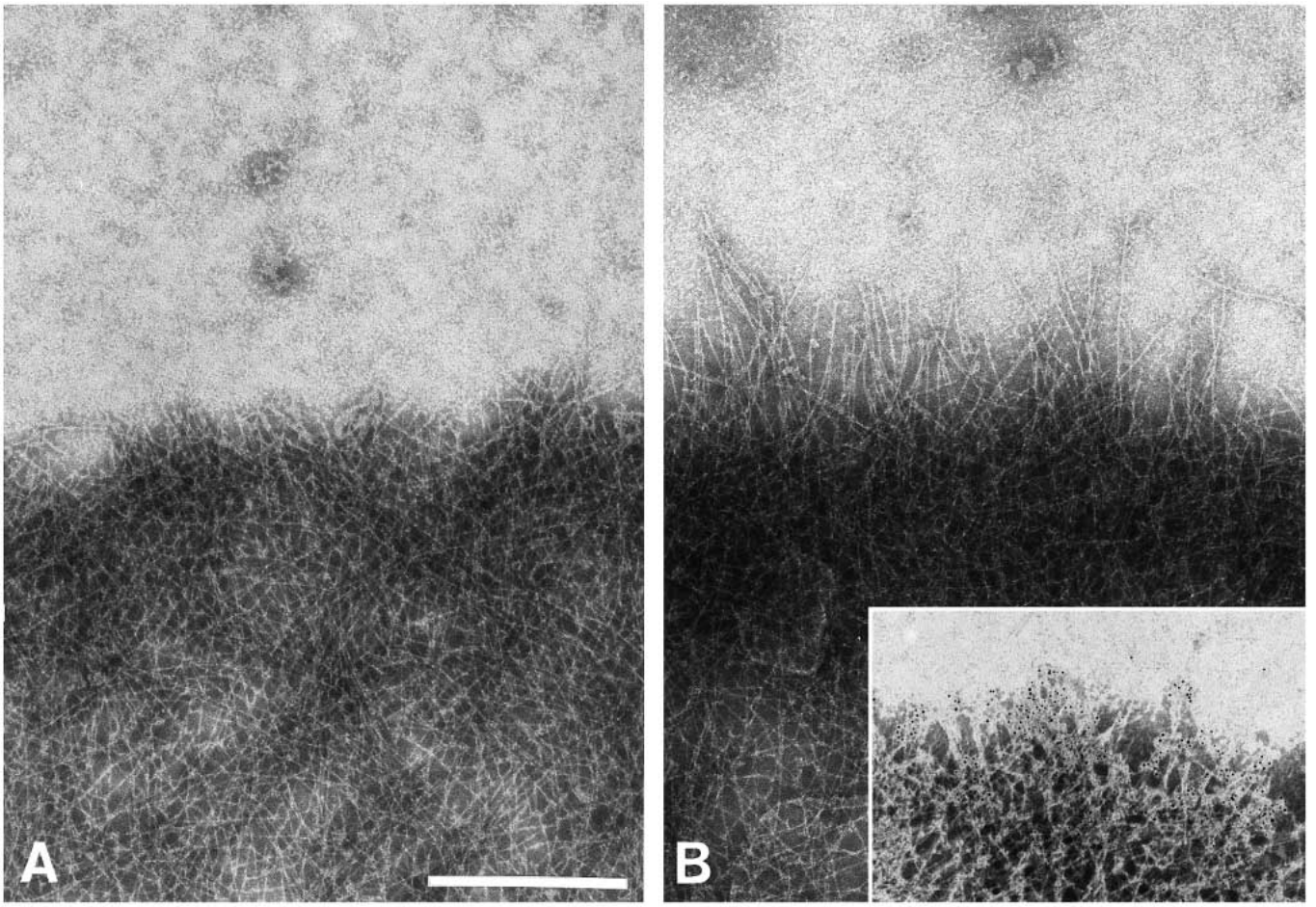

Fig. 8. Exogenous actin incorporates only into preexisting filaments in EGF stimulated MTLn3 cells. Electron micrographs of Triton X-100 permeabilized MTLn3 cells after stimulation with EGF. (A) Incubation with buffer C in the absence of exogenous actin, (B) incubation with 0.45 μM G-actin for 1 minute; (inset) with biotin-actin for 30 seconds followed by staining with anti-biotin colloidal gold. Colloidal gold marks the sites of incorporation of exogenous biotin-actin into the cytoskeleton as the ends of pre-existing (unlabeled) actin filaments. Bar, 0.5 μm.

or without fluorescein-phalloidin, i.e. rhodamine signal was observed around the leading edge and at the end of stress fibers (Fig. 9C arrows). In the presence of cytochalasin D (Fig. 9D) rhodamine-labeled actin incorporation into the EGF-stimulated saponin permeabilized cells is inhibited to the background levels.

To determine whether the addition of rhodamine-labeled actin reflects polymerization or binding of rhodamine-labeled actin oligomers to the permeabilized cell, we investigated whether the nucleation activity was inhibited by pretreatment of lysed cells with 100 nM gelsolin-actin (GA_2) complex, followed by washing out of the unbound GA_2 complex. At 100 nM, the GA_2 concentration of this experiment is 100 times above its K_d (1 nM) for free barbed ends, thus polymerization of rhodamine-labeled actin at the barbed ends should be completely blocked. To confirm this, we measured the capping activity of GA_2 with 0.5 μM F-actin seeds and 2 μM pyrene-labeled actin. Polymerization of 2 μM pyrene-labeled actin is 100% blocked in 100 nM GA_2 pretreated F-actin seeds (data not shown). After the characterization of the GA_2 complex capping activity with F-actin seeds, we measured the capping activity of GA_2 in lysed cells. MTLn3 cells were permeabilized in saponin and phallicidin for 1 minute then incubated with 100 nM GA_2 or 100 nM G-actin for 10 minutes. Free GA_2 and phallicidin was washed off before the addition of 0.45 μM rhodamine-labeled actin which was incubated for various times. The rhodamine-labeled actin fluorescence was at background level for lysed MTLn3 cells that were pretreated with 100 nM GA2 and incubated with 0.45 μM rhodamine-labeled actin for 2 minutes (data not shown)

To observe the incorporation of rhodamine-actin onto pointed ends of lysed MTLn3 cells and to compare the spatial distribution of pointed ends between EGF stimulated and control cells, we pretreated the lysed cells with 100 nM GA_2 or 100 nM G-actin, washed out the unbound GA2 complex and then incubated with 2 μM rhodamine-labeled actin. As shown in Fig. 10, pretreatment of lysed cells with 100 nM GA_2 decreases rhodamine-labeled actin incorporation of EGF

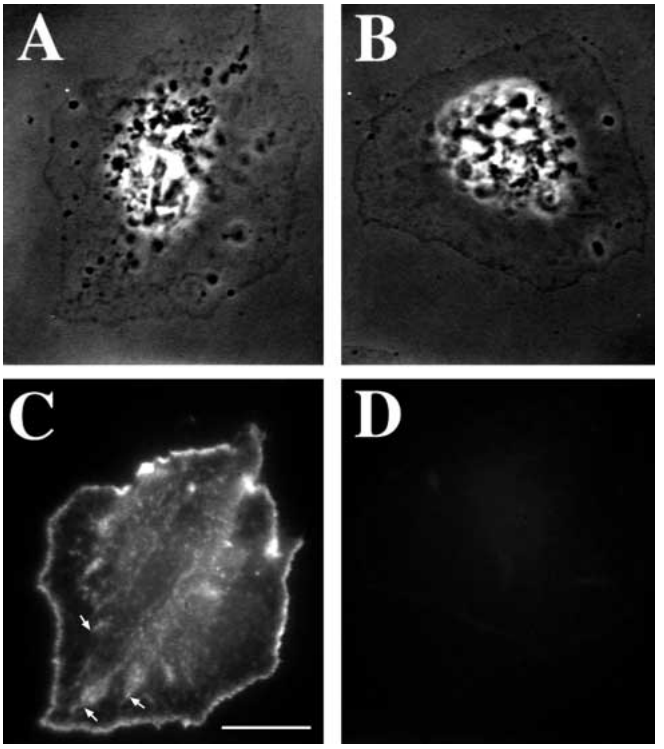

Fig. 9. Cytochalasin D inhibits the incorporation of rhodamine-labeled actin in permeabilized EGF-stimulated MTLn3 cells. Cells were stimulated, permeabilized in the absence (A,C) or presence (B,D) of 100 nM cytochalasin D and then incubated for 5 minutes with rhodamine-labeled actin in permeabilization buffer. To eliminate any cross channel fluorescence, these cells were not stained with fluorescein-phalloidin. Under these conditions the rhodamine-labeled actin image is similar to those seen in preparations also stained with fluorescein-phalloidin. Arrows indicate the rhodamine signal at the end of stress fibers in EGF stimulated cells. No fluorescence was observed in the fluorescein channel (not shown) demonstrating that the fluorescein-phalloidin image is not affected by the rhodamine-labeled actin fluorescence. (A,B) Phase-contrast, and (C,D) rhodamine channel. Bar, 10 μM.

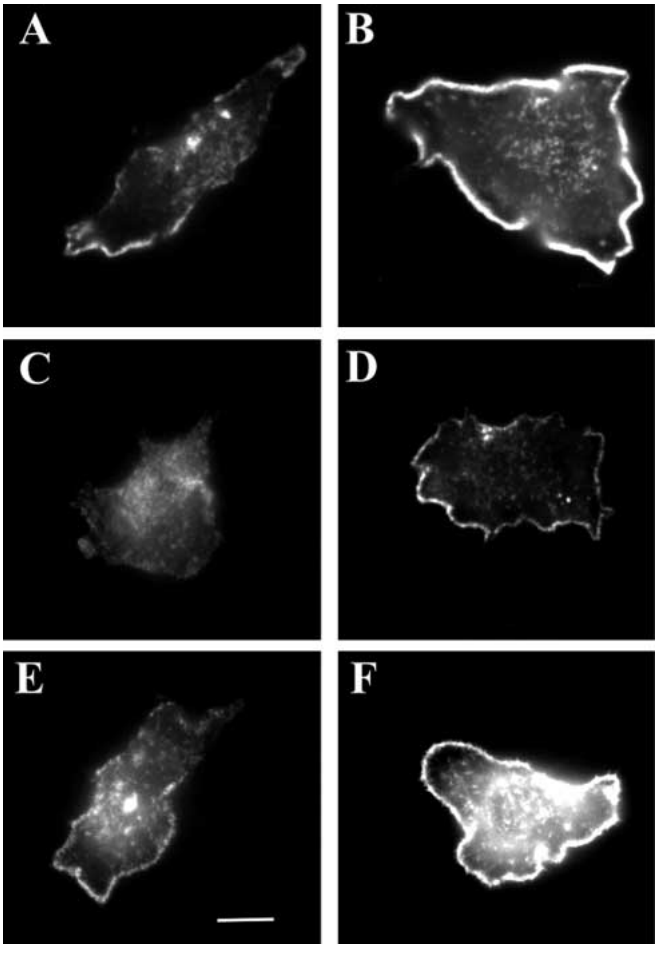

Fig. 10. Rhodamine-labeled actin incorporation is inhibited by pretreatment of saponin permeabilized and phallicidin stabilized MTLn3 cells with 100 nM gelsolin-actin (GA_2) complex. Cells were treated with 5 nM EGF (B,D,F) or buffer (A,C,E) for 1 minute, permeabilized with lysis buffer containing 5 μM of phallicidin for 1 minute and incubated with 100 nM G-actin (A,B), or 100 nM of GA_2 (C-F) for 10 minutes. After 2 washes, 2 μM rhodamine-labeled actin was incubated with cells for 2 minutes (C,D) or 10 minutes (E,F). Bar, 10 μm.

stimulated cells by 8.94±1.34-fold (Fig. 10B,D) and control cells by 6.26±1.33-fold (Fig. 10A,C) compared to parallel samples incubated for 10 minutes in 100 nM G-actin. Pointed end incorporation of rhodamine-labeled actin by the EGF stimulated cells (Fig. 10D) is 2.12±0.47 (n=20) times higher than that of control cells (Fig. 10C). Because of the slower on rate of the pointed ends, incorporation is more apparent after 10 minutes of rhodamine-labeled actin incubation (Fig. 10E, F), a time at which the incubation of rhodamine-labeled actin incorporation was linear (data not shown).

DISCUSSION

EGF stimulates actin nucleation activity in MTLn3 cells

The major result of this study is that stimulation of metastatic MTLn3 cells with EGF causes an increase in actin nucleation activity resulting from the appearance of barbed filament ends at the leading edge of growing lamellipods. Actin nucleation activity that is stimulated by EGF results in actin polymerization that is sensitive to cytochalasin D. Sensitivity to cytochalasin D is observed in cell lysates from both resting and stimulated cells, indicating that the actin filaments in MTLn3 cells are assembled mostly from free barbed ends. However, the background nucleation activity in control cells is small relative to the increase in the nucleation activity in EGF-stimulated cells. The number of barbed ends increases by 1.3×10^4 from 2.4×10^4 to 3.7×10^4 per cell within 1 minute of EGF stimulation, a median value considering the broad range of values that have been measured in other systems. For example, in neutrophils about 2×10^5 new filaments appear within 90 seconds of stimulation with FMLP (Cano et al., 1991), approximately 4×10^4 barbed ends appear within 5 seconds in *Dictyostelium* in response to stimulation with cAMP (J. Han and J. Condeelis, unpublished) and 500 barbed ends appear within 20 seconds following thrombin stimulation of platelets (Hartwig, 1992).

Properties of the EGF stimulated actin nucleation sites in permeabilized MTLn3 cells

Incorporation of rhodamine-labeled actin to permeabilized cells appears to be highly specific for polymerization onto preexisting filament ends in cells, as demonstrated by the following results: (1) rhodamine-labeled actin incorporation in EGF stimulated cells is dependent on the preexisting free barbed ends, as shown by the inhibition of rhodamine-labeled actin signal by cytochalasin D, capping protein, and gelsolin-actin complex; (2) rhodamine-labeled actin incorporation is limited to the tip of the lamellipod and ends of stress fibers; (3) the rhodamine-labeled actin signal increases linearly with time of incubation without a detectable lag period; (4) elongated actin filaments are seen in negatively stained permeabilized cells incubated with exogenous actin only in association with pre-existing actin filaments and never in the background; (5) the ratio of rhodamine-labeled actin to F-actin at the leading edge increases upon EGF stimulation. These results demonstrate that the sites nucleating polymerization are primarily free barbed ends of existing actin filaments in permeabilized MTLn3 cells. Furthermore they argue against the idea that the rhodamine signal observed in the permeabilized MTLn3 cells is due to new filaments that are assembled in the incubation solution which then become cross linked to the permeabilized cell cytoskeleton. The similar overall pattern of actin nucleation kinetics after EGF stimulation for cells in suspension and cells adherent to a surface indicates that the fluorescence of rhodamine-labeled actin observed in the permeabilized cells reflects the actin polymerization of free barbed ends seen in suspended cells as measured using pyrene-labeled actin.

The timing and location of the stimulated actin nucleation activity in MTLn3 cells can account for the observed accumulation of F-actin at the leading edge of extending lamellipods as documented in a previous study of MTLn3 cells (Segall et al., 1996). The finding that the nucleation activity is transient, occurs before the onset of lamellipod extension and is localized to the leading edge supports the hypothesis that extension is caused by localized actin polymerization at the leading edge (Condeelis, 1993; Segall et al., 1996).

EGF stimulates an increase in number of filaments in permeabilized MTLn3 cells

Unlike A431 cells (Rijken et al., 1991) EGF stimulation of MTLn3 cells does not cause a continual increase in cellular F-actin. Rather, EGF stimulates a transient increase in F-actin content. The maximum increase in F-actin content occurs after the peak of nucleation activity suggesting that the increase in the number of barbed ends causes an increase in F-actin content. In the presence of 100 nM cytochalasin D, EGF stimulation induces a decrease in total F-actin content in whole cells. These results predict that EGF stimulates both actin polymerization and depolymerization. The presence of EGF-stimulated depolymerization activity is consistent with the accumulation of F-actin at the leading edge if actin polymerization there exceeds depolymerization compared to other regions of the cell where both reactions may be balanced.

Since the rate of depolymerization is dependent on the number of filaments, the increase in actin depolymerization after EGF simulation suggests that EGF may also stimulate an increase in the number of filaments in MTLn3 cells. To test if there is an increase in the number of actin filaments in MTLn3 cells after EGF stimulation, we measured the relative amount of pointed end incorporation of rhodamine-labeled actin by polymerization of 2 μM rhodamine-labeled actin in permeabilized stimulated and control cells that were pretreated with 100 nM GA_2 to cap all free barbed ends. Pointed end incorporation of rhodamine-labeled actin by the EGF stimulated cells is 2.12±0.47 times higher than that of control cells. Therefore, addition of EGF to MTLn3 cells stimulates an increase in the number of pointed ends, i.e. number of filaments.

Currently, three mechanisms have been postulated to explain the rapid appearance of barbed ends in response to agonist stimulation (Condeelis, 1993; Zigmond, 1996; Schafer et al., 1996). (A) Uncapping of pre-existing filaments leading to an increase in the filament length distribution; (B) de novo nucleation of actin polymerization from a template molecule to form new barbed ends without affecting pre-existing filaments; and (C) severing of pre-existing filaments to form more uncapped filament ends, causing a decrease in the filament length distribution. Mechanism C explains the EGF

stimulated depolymerization of F-actin in the presence of cytochalasin D since EGF-induced severing would shorten the filament length distribution and result in the disappearance of filaments due to rapid pointed end depolymerization if barbed ends could not elongate. In addition, the identical pattern of rhodamine-labeled actin incorporation generated by addition of 0.45 μM rhodamine-labeled actin or 2 μM rhodamine-labeled actin to permeabilized cells, indicate that the barbed and pointed ends occupy the same location within cells within the resolution limit of the light microscope. Since EGF stimulation causes an increase in both barbed and pointed end incorporation of rhodamine-labeled actin in the same location, either severing or de novo nucleation is possible. The increase in the number of pointed ends after EGF stimulation in MTLn3 cells is consistent with other studies where an increase in the number of short filaments in neutrophils and *Dictyostelium* was measured following stimulation (Cano et al., 1990; Eddy et al., 1997).

Mechanism A is consistent with PIP2-mediated uncapping of actin filaments by gelsolin (Hartwig, 1992) and capping protein (Hartwig et al., 1995; Schafer et al., 1996). Both gelsolin, a PIP2-regulated barbed end capping protein which severs and then caps the newly created barbed end (Hartwig, 1992) and capping protein, a heterodimeric barbed end capper that is regulated by PIP2 (Schafer et al., 1996), have been proposed to control the availability of barbed ends by uncapping as PIP2 levels increase in the plasma membrane following stimulation. The location, very close to the plasma membrane of the leading edge, of nucleation sites for rhodamine-labeled actin incorporation is consistent with a role for a phosphoinositol-regulated uncapping mechanism (Hartwig et al., 1995). However, it remains to be established if uncapping of actin filaments is a major mechanism for generating free-barbed ends after agonist stimulation. Gelsolin null cells can mobilize free barbed ends after stimulation (Witke et al., 1995) and conflicting results have been reported concerning whether capping protein is released from actin filaments in intact cells following stimulation as required by mechanism A (Nachmias et al., 1996; Barkalow et al., 1996; Eddy et al., 1997). A simple uncapping mechanism (A) is also inconsistent with the increase in filament number reported here and elsewhere (Cano et al., 1991; Eddy et al., 1997).

The appearance of nucleation sites proximal to the membrane of the leading edge in EGF-stimulated MTLn3 cells as reported here is consistent with previous observations in A431 and Cos-7 cells where accumulation of F-actin following EGF stimulation is proximal to the EGF-receptor in the plasma membrane (Wiegant et al., 1986; Gonzalez et al., 1993) and a report that EGF-R signals PIP2 regulated actin binding proteins like gelsolin (Chen et al., 1996). The significance of co-localization between the EGF-receptor and F-actin is unclear but the conclusions that the EGF-R is itself an actin binding protein (den Hartigh et al., 1992), that F-actin in association with the EGF-R may form an active signaling complex (Diakonova et al., 1995; van Delft et al., 1995) and that actin nucleation sites form immediately adjacent to the plasma membrane after EGF-stimulation as reported here, provide clues for future research.

This work was supported by USAMRDC 2466 (J.S.), GM38511 (J.C.) and a NIH training grant 5 T32 HL07675-07 (A.Y.C). J. Segall is an established scientist of the New York affiliate of the American Heart Association. The authors acknowledge M. Cammer and the AECOM Analytical Imaging Facility for help in image analysis, Jinghua Han for supplying capping protein and John Hartwig for supplying gelsolin.

REFERENCES

Barkalow, K., Witke, W., Kwiatkowski, D. J. and Hartwig, J. H. (1996). Coordinated regulation of platelet actin filament barbed ends by gelsolin and capping protein. *J. Cell Biol.* **134**, 389-399.

Blay, J. and Brown, K. D. (1985). Epidermal growth factor promotes the chemotactic migration of cultured rat intestinal epithelial cells. *J. Cell. Physiol*. **124**, 107-112.

Boonstra, J., Rijken, P., Humbel, B., Cremers, F., Verkleij, A. and van Bergen en Henegouwen, P. (1995). The epidermal growth factor. [Review.] *Cell Biol. Int.* **19**, 413-430.

Cano, M. L., Lauffenburger, D. A. and Zigmond, S. H. (1991). Kinetic analysis of F-actin depolymerization in polymorphonuclear leukocyte lysates indicates that chemoattractant stimulation increases actin filament number without altering the filament length distribution. *J. Cell Biol*. **115**, 677-687.

Carson, M., Weber, A. and Zigmond, S. (1986). An actin-nucleating activity in polymorphonuclear leukocytes is modulated by chemotactic peptides. *J. Cell Biol.* **103**, 2707-2714.

Chen, P., Murphy-Ullrich, J. E. and Wells, A. (1996). A role for gelsolin in actuating epidermal growth factor receptor-mediated cell motility. *J. Cell Biol.* **134**, 689-698.

Condeelis, J. S. (1993). Life at the leading edge: the formation of cell protrusions. [Review.] *Annu. Rev. Cell Biol*. **9**, 411-444.

Cooper, J. A., Walker, S. B. and Pollar, T. D. (1983). Pyrene actin: documentation of the validity of a sensitive assay for actin polymerization. *J. Muscle Res. Cell Motil*. **4**, 253-262.

Dadabay, C. Y., Patton, E., Cooper, J. A. and Pike, L. J. *(*1991). Lack of correlation between changes in polyphosphoinositide levels and actin/gelsolin complexes in A431 cells treated with epidermal growth factor. *J. Cell Biol*. **112**, 1151-1156.

den Hartigh, J. C., van Bergen en Henegouwen, P. M., Verkleij, A. J. and Boonstra, J. (1992). The EGF receptor is an actin-binding protein. *J. Cell Biol*. **119**, 349-355.

Devreotes, P. N. and Zigmond, S. H. (1988). Chemotaxis in eukaryotic cells: a focus on leukocytes and *Dictyostelium*. [Review.] *Annu. Rev. Cell Biol*. **4**, 649-686.

Diakonova, M., Payrastre, B., van Velzen, A. G., Hage, W. J., van Bergen en Henegouwen, P. M., Boonstra, J., Cremers, F. F. and Humbel, B. M. (1995). Epidermal growth factor induces rapid and transient association of phospholipase C-1 with EGF-receptor and filamentous actin at membrane ruffles of A431 cells. *J. Cell Sci.* **108**, 2499-2509.

Eddy, R. J., Han, J. H., Sauterer, R. A. and Condeelis, J. S. (1996). A major agonist-related capping activity in Dictyostelium is due to the capping protein, cap 32/34. *Biochem. Biophys. Acta* **1314**, 247-259.

Eddy, R. J., Han, J. and Condeelis, J. S. (1997). Capping protein terminates but does not initiate chemoattractant-induced actin assembly in *Dictyostelium*. *J. Cell Biol.* **139** (in press).

Gonzalez, F. A., Seth, A., Raden, D. L., Bowman, D. S., Fay, F. S. and Davis, R. J. (1993). Serum-induced translocation of mitogen-activated protein kinase to the cell surface ruffling membrane and nucleus. *J. Cell Biol.* **122**, 1089-1101.

Grotendorst, G. R., Soma, Y., Takehara, K. and Charette, M. (1989). EGF and TGF-alpha are potent chemoattractants for endothelial cells and EGF-like peptides are present at sites of tissue regeneration. *J. Cell. Physiol*. **139**, 617-623.

Hall, A. L., Warren, V., Dharmawardhane, S. and Condeelis, J. (1989). Identification of actin nucleation activity and polymerization inhibitor in ameboid cells: their regulation chemotactic stimulation. *J. Cell Biol.* **109**, 2207-2213.

Hartwig, J. H. (1992). Mechanisms of actin rearrangements mediating platelet activation. *J. Cell Biol*. **118**, 1421-1442.

Hartwig, J. H., Bokoch, G. M., Carpenter, C. L., Janmey, P. A., Taylor, L. A., Toker, A. and Stossel, T. P. (1995). Thrombin receptor ligation and activated Rac uncap actin filament barbed ends through phosphoinositide synthesis in permeabilized human platelets. *Cell* **82**, 643-653.

Hoelting, T., Siperstein, A. E., Clark, O. H. and Duh, Q. Y. (1994).

Epidermal growth factor enhances proliferation, migration, and invasion of follicular and papillary thyroid cancer in vitro and in vivo. *J. Clin. Endocr. Metab*. **79**, 401-408.

Kaufmann, A. M., Khazaie, K., Wiedemuth, M., Rohde-Schulz, B., Ullrich, A., Schirrmacher, V. and Lichtner, R. B. (1990). Expression of epidermal growth factor receptor correlates with metastatic potential of 13762 NF rat mammary adenocarcinoma cells. *Int. J. Oncol*. **4**, 1149-1155.

Lichtner, R. B., Wiedemuth, M., Kittmann, A., Ullrich, A., Schirrmacher, V. and Khazaie, K. (1992). Ligand-induced activation of epidermal growth factor receptor in intact rat mammary adenocarcinoma cells without detectable receptor phosphorylation. *J. Biol. Chem*. **267**, 11872-11880.

Nachmias, V. T., Golla, R., Casella, J. F, and Barron-Casella, E. (1996). Cap Z, a calcium insensitive capping protein in resting and activated platelets. *FEBS Lett*. **378**, 258-262.

Neri, A., Welch, D., Kawaguchi, T. and Nicolson, G. L. (1982). Development and biologic properties of malignant cell sublines and clones of a spontaneously metastasizing rat mammary adenocarcinoma. *J. Nat. Cancer Inst*. **68**, 507-517.

Pedersen, P. H., Ness, G. O., Engebraaten, O., Bjerkvig, R., Lillehaug, J. R., and Laerum, O. D. (1994). Heterogeneous response to the growth factors [EGF, PDGF (bb), TGF-alpha, bFGF, IL-2] on glioma spheroid growth, migration and invasion. *Int. J. Cancer* **56**, 255-261.

Peppelenbosch, M. P., Tertoolen, L. G., Hage, W. J. and de Laat, S. W. (1993). Epidermal growth factor-induced actin remodeling is regulated by 5-lipoxygenase and cyclooxygenase products. *Cell* **74**, 565-575.

Pollard, T. D. (1986). Rate constants for the reactions of ATP- and ADP-actin with the ends of actin filaments. *J. Cell Biol*. **103**, 2747-2754.

Price, J. E., Sauder, D. N. and Fidler, I. J. (1988). Tumorigenicity and metastatic behavior in nude mice of two human squamous cell carcinoma lines that differ in production of cytokine ETAF/IL-1. *J. Invest. Dermatol*. **91**, 258-262.

Redmond, T. and Zigmond, S. H. (1993). Distribution of F-actin elongation sites in lysed polymorphonuclear leukocytes parallels the distribution of endogenous F-actin. *Cell Motil. Cytoskel*. **26**, 7-18.

Rijken, P. J., Hage, W. J., van Bergen en Henegouwen, P. M., Verkleij, A. J. and Boonstra, J. (1991). Epidermal growth factor induces rapid reorganization of the actin microfilament system in human A431 cells. *J. Cell Sci*. **100**, 491-499.

Rijken, P. J., Post, S. M., Hage, W. J., van Bergen en Henegouwen, P. M., Verkleij, A. J. and Boonstra, J. (1995). Actin polymerization localizes to the activated epidermal growth factor receptor in the plasma membrane, independent of the cytosolic free calcium transient. *Exp. Cell Res*. **218**, 223-232.

Royce, L. S. and Baum, B. J. (1991). Physiologic levels of salivary epidermal growth factor stimulate migration of an oral epithelial cell line. *Biochim. Biophys. Acta* **1092**, 401-403.

Schafer, D. A., Jennings, P. B. and Cooper, J. A. (1996). Dynamics of capping protein and actin assembly in vitro: uncapping barbed ends by PIP2. *J. Cell Biol*. **135**, 169-179.

Segall, J. E., Tyerech, S., Boselli, L., Masseling, S., Helft, J., Chan, A. Y., Jones, J. and Condeelis, J. (1996). EGF stimulates lamellipod extension in metastatic mammary adenocarcinoma cells by an actin-dependent mechanism. *Clin. Exp. Metast.* **14**, 61-72.

Silletti, S. and Raz, A. (1993). Autocrine motility factor is a growth factor. *Biochem. Biophys. Res. Commun*. **194**, 446-457.

Spudich, J. A. and Watt, S. (1971). The regulation of rabbit muscle contraction. I. Biochemical studies of the interaction of the tropomyosin-troponin complex with actin and the proteolytic fragments of myosin. *J. Biol. Chem*. **246**, 4866-4871.

Stracke, M., Liotta, L. A. and Schiffmann, E. (1993). The role of autotaxin and other motility stimulating factors in the regulation of tumor cell motility. *Symp. Soc. Exp. Biol*. **47**, 197-214.

Symons, M. H. and Mitchison, T. J. (1991). Control of actin polymerization in live and permeabilized fibroblasts. *J. Cell Biol*. **114**, 503-513.

van Delft, S., Verkleij, A. J., Boonstra, J. and van Bergen en Henegouwen, P. M. *(*1995). Epidermal growth factor induces serine phosphorylation of actin. *FEBS Lett*. **357**, 251-254.

Wang, X., Kamiyama, K., Iguchi, I., Kita, M. and Imanishi, J. (1994). Enhancement of fibronectin-induced migration of corneal epithelial cells by cytokines. *Invest. Ophthalmol. Vis. Sci*. **35**, 4001-4007.

Welch, D. R., Neri, A. and Nicolson, G. L. (1983). Comparison of 'spontaneous' and 'experimental' metastasis using rate 13762 mammary adenocarcinoma metastatic cell clones. *Inv. Metast.* **3**, 65-80.

Wiegant, F. A., Blok, F. J., Defize, L. H., Linnemans, W. A., Verkley, A. J., and Boonstra, J. (1986). Epidermal growth factor receptors associated to cytoskeletal elements of epidermoid carcinoma (A431) cells. *J. Cell Biol*. **103**, 87-94.

Witke, W., Sharpe, A. H., Hartwig, J. H., Azuma, T., Stossel, T. P. and Kwiatkowski, D. J. (1995). Hemostatic, inflammatory, and fibroblast responses are blunted in mice lacking gelsolin. *Cell* **81**, 41-51.

Zigmond, S. H. (1996). Signal transduction and actin filament organization. *Curr. Opin. Cell Biol*. **8**, 66-73.